The Scalar Field Dark Matter Model: A Braneworld Connection

Tonatiuh Matos[1], Luis Arturo Ureña-López[2], Miguel Alcubierre[3], Ricardo Becerril[4], Francisco S. Guzmán[5], and Darío Núñez[3]

[1] Centro de Investigación y de Estudios Avanzados del I.P.N, A.P. 14-740, 07000 D.F., México. tmatos@fis.cinvestav.mx

[2] Instituto de Física de la Universidad de Guanajuato, A.P. E-143, 37150, León, Guanajuato, México. lurena@fisica.ugto.mx

[3] Instituto de Ciencias Nucleares, Universidad Nacional Autónoma de México, A.P. 70-543, 04510 México, D.F., México. malcubi@nuclecu.unam.mx, nunez@nuclecu.unam.mx

[4] Instituto de Física y Matemáticas, Universidad Michoacana, Edif. C-3, Ciudad Universitaria 58040, Morelia, Michoacán, México. becerril@ifm1.ifm.umich.mx

[5] Max Planck Institut für Gravitationsphysik, Albert Einstein Institut, Am Müehlenberg 1, 14476 Golm, Germany. guzman@aei-potsdam.mpg.de

Abstract. This work is a review for the progress of the scalar field dark matter (SFDM) hypothesis. Here we outline a possible brane world model justifying the hypothesis of the scalar field origin for the dark matter (DM). This model contains two branes, on one of the branes lives the matter of the standard model of particles but on the other one, only spin-0 fundamental interactions are present. In this model these spin-0 fields are the DM and maybe the dark energy (DE). Thus, DM and DE interact only through the gravitational force with the matter brane. Starting with this hypothesis, we write a Lagrangian where the dark matter is of scalar origin with a cosh scalar field potential. The scalar field with a cosh potential behaves exactly in the same way as dust at cosmological scales. In this sense the scalar field mimics very well cold dark matter (CDM). The free parameters of the Lagrangian can be fixed using cosmological observations. After fixing all the free parameters of the model, we found that a scalar field fluctuation collapses forming objects with a preferred mass of $\sim 10^{12} M_\odot$. Nevertheless, at galactic scales there exist some strong differences with the CDM paradigm. The scalar field contains an effective pression which avoids the collapse of a scalar field fluctuation, implying that scalar field objects like galaxies contain a flat density profile in the center. This implies that the SFDM paradigm could resolve the cusp density profile problem of galaxies.

1 Introduction

The clarification of the origin of the dark matter in the universe is doubtless one of the most important challenges for theoretical physics and cosmology at the present time. Several models have been proposed to get a possible answer, but at some point they seem to have serious flaws. At the present time, the best model we have is the so called Lambda Cold Dark Matter

T. Matos, L.A. Ureña-López, M. Alcubierre, R. Becerril, F.S. Guzmán, and D. Núñez, The Scalar Field Dark Matter Model: A Braneworld Connection, Lect. Notes Phys. **646**, 401–420 (2004)
http://www.springerlink.com/

model (ΛCDM) [1, 2, 3], which can be considered as the standard cosmological model. The most recent observations of the WMAP satellite [2] confirm that stars and dust (made of baryons) represent something like 4% of the whole energy density of the universe; this amount of baryonic matter is in concordance with the limits imposed by nucleosynthesis. The new measurements of the neutrino mass indicate that neutrinos contribute with less than 0.2% of the whole matter. As the WMAP observations also confirm that our universe is flat, then we should admit that most of the matter content of the cosmos is of unknown nature. In other words, the matter component has the following contributions, $\Omega_{\rm M} = \Omega_b + \Omega_\nu + \cdots + \Omega_{\rm CDM} \sim 0.04 + \Omega_{\rm CDM} \sim 0.27$, where $\Omega_{\rm CDM}$ represents the *cold dark matter* (CDM) part of the contributions, which implies $\Omega_{\rm CDM} \sim 0.23$. Even at this point, we are still missing matter as required for a flat universe. The next breakpoint came with the observations of supernovae type Ia [4], which indicate an actual accelerated expansion of the cosmos. The simplest explanation is to introduce the existence of some vacuum energy (also generically called *dark energy*), in the form of a cosmological constant Λ. Then, the ΛCDM model considers a flat universe ($\Omega_\Lambda + \Omega_{\rm M} \approx 1$) containing 96% of unknown matter.

The dark matter candidates in the ΛCDM model are the WIMP's, (Weakly Interacting Massive Particles), most of them being supersymmetric particles. WIMP's behave as dust particles, i.e., as a (cold) pressureless fluid, and then they are very appropriate for the cosmological scales. However, CDM seems not to be completely appropriate at galactic scales. High resolution numerical simulations show that dust fluids follow the Navarro-Frenk-White (NFW) density profile [5] $\varrho_{\rm NFW} \sim 1/[r(r+b)^2]$ for galaxies, which is singular at $r \to 0$. This fact disagrees with recent observations on LSB galaxies [6, 7], showing that the density profile of the dark matter in the center of galaxies seems to be flat $\varrho_{\rm obs}(r \to 0) \sim$ const. rather than cusp. Also, CDM seems to predict an excess of subgalactic structure [8, 9], an excess that has not been detected at all.

There are some arguments stating that such disagreements are not fundamental. For example, it could be that actual telescopes have not enough resolution to see the dark matter density cusp in the center of galaxies due to baryonic dust or something else. Also, the excess of subgalactic structure could be made only of CDM, and then we cannot see them because they do not have baryonic matter at all [10]. Maybe, it is a matter of time that we will find the right CDM physics and the disagreements will disappear. However, it can also be argued that these disagreements between theory and observations could be because we do not have the right candidate for CDM. This is the reason we propose to look for other candidates which could give us all the successful predictions of ΛCDM at cosmological scales, and the right behavior at galactic scales.

As a motivation for the present work, let us start with the following reasoning. In the actual status of our understanding of the universe, there is an apparent asymmetry in the kind of interactions that take part in Nature. The known fundamental interactions are either spin-1, or spin-2. Electromagnetic, weak and strong interactions are spin-1 interactions, while gravitational interactions are spin-2. Of course, this could be just a coincidence. Nevertheless, we know that the simplest particles are the spin-0 ones. The asymmetry lies in the fact that there is no spin-0 fundamental interactions. Why did Nature forget to use spin-0 fundamental interactions? On the other hand, we know from the success of the ΛCDM model that two fields currently take the main role in the Cosmos, the *dark matter* and the *dark energy*. Recently, we have indeed proposed that dark matter is a scalar field, that is, a spin-0 fundamental interaction. This is the so called *Scalar Field Dark Matter* (SFDM) hypothesis [11, 12, 13, 14]. If true, this hypothesis could solve the problem of the apparent asymmetry in our picture of nature.

Let us go further. All unification theories which try to unify gravitation with the rest of the interactions always contain scalar fields. For instance, in brane theory there is a scalar field, the radion, that must be stabilized, and then this scalar field must be endowed somehow with a scalar field potential with a minimum. This point discards that the scalar field could be identified with the dark energy, because a dark energy scalar field (the so called Quintessence), must be running away when the dark energy dominates [15, 16, 17], its potential must be exponential–like, without a minimum. On the other hand, we know that the scalar field with a scalar field potential containing a minimum sometimes behaves as a dust fluid [6]. From the ΛCDM model, we expect the dark matter to behave as a dust fluid at cosmic scales [1]. Then, the radion or some scalar field of this theory could be identified with the dark matter.

Second, it is known that a exponential–like scalar field potential fits very well the constraints from big bang nucleosynthesis, due to its (so called) tracker solutions [15, 16, 18], and then fine tunning can be avoided. The most simple example of a potential with both exponential behavior and a minimum is a cosh potential.

And third, the anisotropies of the CMB suggest that the universe should have had an early inflationary epoch in order to solve the horizon and the flatness problem, among others. Recently, braneworld scenarios [19, 20], where a 3-brane hypersurface represents our observable universe, have attracted a lot of interest [21, 22, 23, 24, 25, 26, 27, 28]. Originally proposed to solve the hierarchy problem, this kind of ideas have been applied to cosmology where they can be confronted to astronomical observations. In *brane cosmology*, the Friedmann equation (see (12) below) contains an extra quadratic density term, which permits inflation to occur even in the cases not permitted within standard cosmology [29]. As the universe expands, the quadratic term of the density in the Friedmann equation becomes negligible and then inflation comes to an end while at the same time the dynamics of stan-

[6] The existence of a minimum is a necessary condition but not a sufficient one, see [17]

dard cosmology is recovered. Furthermore, it is possible for the inflaton field to survive and become part of the dark matter at late times [29, 30, 31, 32].

This paper is organized as follows. In Sect. 2 we propose a consistent model of inflationary dark matter within the so called braneworld model. In Sect. 3 we study the standard cosmology for the surviving radion field, and in Sect. 4 we discuss the behavior of this scalar field at galactic level and the issue of structure formation under the SFDM hypothesis. Finally in Sect. 5 we give some conclusions.

2 Scalar Field Matter from Brane Cosmology

A series of theories and models like the superstring theory, have shown certain success as fundamental theories. The main feature they show is the existence of many scalar fields called dilatons, inflatons, radions, etc., depending on the type of fields they are coupled to. Nevertheless, fundamental scalar fields have not been observed in nature, and then this fundamental theories should postulate a mechanism to decouple those scalar fields at some point in the history of the universe.

Using the previous analysis, we start with a model which contains two branes [33], as in the Randal-Sundrum (RS) model. Like in the RS model, we suppose that in one of the branes lives the matter of the standard model of particles, in this brane the fundamental interactions are all of them of spin-1. The difference is that we suppose that in the other brane lives a set of fundamental spin-0 interactions which interact only through the gravitational interaction on the bulk with the first brane. Of course, we suppose that in this second brane, with only spin-0 fundamental interactions, lives the dark matter and maybe the dark energy, if it is modelled by Quintessence. This could explain why we are not able to see the dark matter, because it is living in the other brane, but we are able to feel it, because it acts through the gravitational interactions with our brane (see [33] for a extended explanation). This is also the reason why we cannot see spin-0 fundamental interactions in the universe. They determine the structure and maybe the behavior of the universe, but they live in the other brane, we cannot detect them, we can only feel them through their gravitation. The universe is then, a higher-dimensional manifold, which contains two three-dimensional submanifolds, i.e., two branes. In one of them there are only spin-0 fundamental interactions while in the other one there are only spin-1 fundamental interactions. In the higher-dimensional manifold the fundamental interaction is the gravitational one, i.e., the spin-2 interaction. Our brane, with only spin-1 fundamental interactions, lives very close to the other brane, feeling its presence, but not being able to see it at all. Then, in our brane, the dark matter can be modelled effectively using a scalar feel Lagrangian in the main action. In the next section we see that this model contains some very nice features.

2.1 Brane World Scalar Field Dynamics

The effective action describing the scalar field dynamics in the brane world paradigm can be obtained from the following Lagrangian

$$S = \int dx^4 dy \sqrt{-G}\,(R + \Lambda) + \int dx^4 \sqrt{-g}\left(\lambda_{\mathrm{b}} - \frac{1}{2}(\partial\Phi)^2 - V(\Phi)\right) , \tag{1}$$

where

$$V(\Phi) = V_0\left[\cosh(\sqrt{\kappa_0}\lambda\Phi) - 1\right] , \tag{2}$$

is a convenient potential for the scalar field and λ_{b} is the brane tension. The 5-dimensional metric can be written as

$$dS_5^2 = -A_{\pm} d\tau^2 + A_{\pm}^{-1} da^2 + a^2 d\Omega_3^2 , \tag{3}$$

$$A_{\pm} = \kappa_l - \frac{\Lambda^{\pm}}{6}a^2 - \frac{2\mathcal{M}^{\pm}}{M_{(5)}^3 a^2} , \tag{4}$$

being κ_l an integrations constant. In the cosmic time gauge the 4-dimensional inherited metric of the brane is

$$dS_4^2 = -dt^2 + a^2 d\Omega_3^2 . \tag{5}$$

The relevant equations of motion for the model are the following

$$\left(\dot{a}^2 + A_-\right)^{1/2} - \left(\dot{a}^2 + A_+\right)^{1/2} = \frac{\kappa_5 a \rho}{3} , \tag{6}$$

$$\dot{\rho} + 3\frac{\dot{a}}{a}(\rho + P) = 0 . \tag{7}$$

where κ_5 is the five dimensional gravitational constant. The last equation represents the energy-momentum conservation on the brane. Here P is the total pressure and ρ is the total energy density. If we assume that $\Phi = \Phi(t)$, the scalar field energy and pressure are expressed respectively as

$$\varrho_\Phi = \frac{1}{2}\dot{\Phi}^2 + V(\Phi) , \tag{8}$$

$$p_\Phi = \frac{1}{2}\dot{\Phi}^2 - V(\Phi) . \tag{9}$$

These equations can be cast as

$$\dot{a}^2 + \frac{1}{2}(A_+ + A_-) = \frac{3}{4}\kappa_5^2 a^2 \varrho^2 + \left(\frac{3}{2\kappa_5 a \varrho}\right)^2 (A_+ - A_-)^2 , \tag{10}$$

where $\rho = \varrho_\Phi + \lambda_{\mathrm{b}}$. For Z_2 symmetry the former equation can be written in the following way

$$H^2 = \frac{\dot{a}^2}{a^2} = \frac{-\kappa_l^2}{a^2} + \frac{3}{2}\kappa_5^2\lambda\varrho_\Phi(1+\varrho_\Phi/2\lambda_\mathrm{b}) + \frac{\Lambda}{6} + \frac{3}{4}\kappa_5^2\lambda_\mathrm{b}^2 + \frac{2\mathcal{M}}{M_{(5)}^3 a^4} \,. \tag{11}$$

For flat geometry ($\kappa_l = 0$) and vanishing $\mathcal{M}$ we get

$$H^2 = \frac{3}{2}\kappa_5^2\lambda_\mathrm{b}\varrho_\Phi(1+\varrho_\Phi/2\lambda_\mathrm{b}) + \frac{\Lambda}{6} \,. \tag{12}$$

Einstein cosmology in four-dimensions is recovered when the brane tension is significantly higher than energy density $\lambda_\mathrm{b} \gg \varrho_\Phi$. The quadratic correction is important at high energies and means that the expansion rate is increased with respect to the standard Einstein cosmology. Analysis of the dynamics of this system has been done in [36, 29, 30, 31, 32, 38].

If we were interested in a zero effective cosmological constant Λ we would require fine-tuning, but the changes to the former analysis would be negligible.

2.2 Inflation in the Braneworld Scenario

The appealing feature of the braneworld model described above is that it inspired new ideas about inflationary cosmology, which would have taken place in the high-energy regime of (12) corresponding to the early universe. Under quite general conditions, there is an extra-friction induced on the KG equation due to the quadratic density term in (12). This allows for the existence of inflationary solutions for *steep* scalar field potentials, which are otherwise not capable of supporting inflation in standard cosmology[29, 30, 31].

We assume that the scalar (inflaton) field Φ was initially displaced from the global minimum of its cosh potential, $\kappa_0\lambda^2\Phi^2 \gg 1$, which is a reasonable assumption if we think of the high energy scales of the very early universe. In this limit, the potential (2) can be approximated by an exponential function. Braneworld inflation driven by such a potential has been studied in [29, 31, 32].

Recalling the main results, the COBE normalization of the cosmic microwave background (CMB) power spectrum relates the value of the brane tension to the scalar field self–coupling such that $\lambda_\mathrm{b}^{1/4}\lambda^{3/2} \approx 10^{15}$ GeV. For the favored value of the latter, as implied by (21) below, we deduce that

$$\lambda_\mathrm{b} \simeq \left(6 \times 10^{-7} M_4\right)^4 = 2.88 \times 10^{51}\,\mathrm{GeV}^4 \,. \tag{13}$$

For these given values of $\{\lambda, \lambda_\mathrm{b}\}$, the magnitude of the potential energy at the end of inflation is $V_\mathrm{end} \simeq (3.2\times10^{-6}M_4)^4 = 2.33\times10^{54}\,\mathrm{GeV}^4$ and this implies that $\Phi_\mathrm{end} \approx 2M_4$, thus justifying the exponential approximation during the inflationary era.

An important inflationary parameter is the spectral index n_s of the scalar fluctuation spectrum, which is given by to be [31]

$$n_{\rm s} = 1 - \frac{4}{N+1} = 0.94 \; , \tag{14}$$

where $N \approx 70$ is the number of e-foldings that elapse between the epoch that a given observable mode crosses the Hubble radius during inflation and the end of the inflationary epoch. Remarkably, the tilt of the scalar perturbation spectrum in this scenario is *uniquely* determined by the number of e–foldings and is *independent* of the parameters in the potential (2). Furthermore, the amplitude of the primordial gravitational wave spectrum, A_T, relative to that of the density perturbations, A_S, can be estimated as [29]

$$r = 4\pi \frac{A_T^2}{A_S^2} \simeq 0.4 \tag{15}$$

implying after COBE normalization that $A_T^2 \approx 1.7 \times 10^{-10}$. This ratio is also independent of the model's parameters and is within the projected sensitivity of the Planck satellite. It provides a potentially powerful test of the model.

Inflation ends when the quadratic corrections to the Friedmann equation (12) become negligible. Due to the steep nature of its potential, the inflaton then behaves as a massless field, where its energy density redshifts as $\varrho_\Phi \propto a^{-6}$. For the reheating of the universe after inflation, we can think of different mechanisms. One first option would be reheating via gravitational particle production due to the time–variation of the gravitational field [37].

However, there are some caveats of the model that should be mentioned. First, the tilted spectral index (14) is at variance with current observations of the CMB anisotropies [2], which favor a flat spectral index $n_{\rm s} \simeq 1$. Second, there is an excess of gravitational waves produced between the end of inflation and the expected recovering of standard cosmology that the latter is not recovered at all. After inflation we have a gravitational waves dominated universe, which seems to be a typical feature of these models[31].

Fortunately, these caveats can be cured if we consider the existence of another scalar field within the so called *curvaton* hypothesis [38]. Such another scalar field is not rare since most super theories consider the existence of more than one scalar field. The curvaton field takes the main role for the predictions, and then both a flat $n_{\rm s}$ and a low density of gravitational waves can be achieved. Moreover, the universe is reheated through the decay of the curvaton field, which is a more efficient reheating mechanism than gravitational particle production.

Notice then that, even within the curvaton hypothesis, the decay of the inflaton field after inflation is not a necessary condition for reheating to occur. This implies that the inflaton field can survive until late times to play other roles in the evolution of the universe, like being part of the missing (dark) matter revealed by observations. In particular, we describe here how the inflaton field associated to the potential (2) could become the CDM at late times[30, 31, 32].

3 Scalar Field Dark Matter in the Cosmological Context

As we mentioned before, the CDM model has become a paradigm for the missing matter responsible for the formation of the large scale structure in the universe, from galaxies to clusters of galaxies. In this respect, we can determine the values of the free parameters of a scalar field dark matter model by comparing its evolution to CDM. Such comparison should be done also at the level of linear perturbations. The latter are important, since we should recover the successful picture of structure formation of CDM, in which primordial perturbations grow by means of gravitational instability.

As mentioned in a previous section, after inflation, we expect to recover the standard Big Bang scenario in which nucleosynthesis can proceed successfully, as suggested by observations and the Standard Model of Particles. This occurs during the epoch of radiation domination, in which the scalar field dark matter evolves with an effective exponential potential. The coexistence of the two fluids, radiation and scalar field, is restricted by a successful nucleosynthesis scenario. The ratio of the scalar field (ϱ_Φ) and radiation (ϱ_γ) energy densities at that time should be [18]

$$\frac{\varrho_\Phi}{\varrho_\gamma} = \frac{4}{\lambda^2 - 4} < 0.2 \, . \tag{16}$$

Observe that the ratio is a constant determined uniquely by the self-coupling λ, that indicates that the scalar field evolves, along its attractor solution, as radiation.

After that, the scalar field reaches the minimum of its potential, and starts to oscillate around it so rapidly that the universe only feels the average energy density and pressure of the field. In fact it can be shown that

$$< \varrho_\Phi > \simeq \varrho_{\mathrm{CDM}} \, , \tag{17}$$

and then the scalar field evolves now as pressureless matter, $< p_\Phi > \simeq 0$ [17, 14, 39, 12, 40, 41]. In order to have a scalar field dark matter model equivalent to CDM at cosmic scales, it is required that the free parameters of the cosh potential obey the following relation,

$$\kappa_0 V_0 \simeq \frac{1.7}{3} \left(\lambda^2 - 4\right)^3 \left(\frac{\Omega_{0\mathrm{CDM}}}{\Omega_{0\gamma}}\right)^3 \Omega_{0\mathrm{CDM}} H_0^2 \, , \tag{18}$$

where $\Omega_{0\mathrm{i}}$ is the current density parameter of the ith-matter component.

Equation (18) shows the allowed values of $\{\lambda \, , V_0\}$ to have an appropriate model of scalar dark matter, one that can mimic the standard CDM model. Up to now, the parameters of the cosh potential cannot be determined uniquely, but more information is necessary. As we shall see below, such information can be taken from the theory of linear perturbations.

3.1 Damping of the Scalar Power Spectrum

As more and new cosmological observations are appearing, it is always a must to check whether the correspondence between SFDM and CDM is preserved at the level of linear perturbations, where CDM is very successful.

When a detailed analysis of scalar perturbations is made [12, 40], it is found that the processed mass power spectrum for the SFDM, in the linear regime, is much the same as the CDM spectrum. Actually, the two spectra are related through the formula[39]

$$P_\Phi(k) = \left[\frac{\cos(x^3)}{1+x^8} \right]^2 P_{\mathrm{CDM}}(k) \,, \tag{19}$$

where $x = k/k_{\mathrm{c}}$, with k the wave number of the different cosmological scales involved in the analysis. k_{c} corresponds to a cutoff scale below which linear perturbations are highly suppressed, and whose value is given by

$$k_{\mathrm{c}} \simeq 1.3\,\lambda\,\sqrt{\lambda^2-4}\,\frac{\Omega_{0\mathrm{CDM}}}{\sqrt{\Omega_{0\gamma}}}\,H_0 \,. \tag{20}$$

If we take a cut-off of the mass power spectrum at $k_{\mathrm{c}} = 4.5\,h\,\mathrm{Mpc}^{-1}$[8], we find that

$$\begin{aligned} \lambda &\simeq 20.3, \\ V_0 &\simeq \left(3.0 \times 10^{-27}\,m_{\mathrm{Pl}} \simeq 36.5\,\mathrm{eV}\right)^4 , \\ m_\Phi &\simeq 9.1 \times 10^{-52}\,m_{\mathrm{Pl}} \simeq 1.1 \times 10^{-23}\,\mathrm{eV}. \end{aligned} \tag{21}$$

All parameters of potential (2) are now completely determined.

We would like to mention that the results shown in (21) are not unchangeable, since the cutoff scale k_{c} could take a larger value; in fact, the larger the cutoff wavenumber value the more similar the SFDM is to the CDM model. However, it is worth to mention that the free parameters of the particular model (2) can be determined from cosmological observations only. As we shall see below, the values in (21) seem to be the appropriate ones for the model to fulfill the requisites of non-linear structure formation.

4 Scalar Field Dark Matter and Structure Formation

At galactic scale, the CDM paradigm predicts a density profile which corresponds to the Navarro-Frenk-White (NFW) profile [5] given by

$$\varrho_{NFW} = \frac{\varrho_0}{(r/r_0)(r/r_0+1)^2} \,, \tag{22}$$

where r is the radial coordinate and r_0 is a parameter. However, this profile seems to have some differences with the inferred profiles from observations on

LSB galaxies[6]. The evidence points to the fact that, in the central regions, galaxies prefer to follow an almost constant density profile. The point is that the NFW model has the support of N-body simulations and has proved to be consistent with observations at cosmic scales, whereas the new observations have no cosmic counterpart that could support them, and it is here where the SFDM shows some advantages with respect to NFW as shown below [9].

The formation of galaxies through gravitational collapse of dark matter is not an easy problem to understand. A good model for galaxy formation has to take into account all the observed features of real galaxies. For example, it seems that many disk galaxies contain a black hole in their center, but others do not [42]. Typical galaxies are spiral, elliptical or dwarf galaxies (irregular galaxies may be galaxies still evolving). In most spiral and elliptical galaxies the luminous matter extends to $\sim 10-30\,\mathrm{kpc}$, and the total content of matter (including dark matter) is of the order of $10^{10}-10^{12}\,\mathrm{M}_\odot$, with about 10 times more dark matter than luminous component. The central density profile of the dark matter in galaxies should not be cusp[43]. Even though the luminous matter is only a small fraction of the total amount of matter in galaxies, it plays an important role in galaxy formation and stability, etc.

Let us now draw the general picture for the gravitational collapse of a scalar field. It is known that the final stage of a collapsed scalar field could be a massive object made of scalar field particles in quantum coherent states, like boson stars (for a complex scalar field) or oscillatons (for a real scalar field) [44, 45]. It is thus important to investigate whether the scalar field would collapse to form structures of the size of galaxies and provide the correct properties of any galactic dark matter candidate, like growing rotation curves and appropriate dark matter distribution functions. Also, we need to know which are the conditions that must be imposed on the scalar field particles.

For instance, axions are massive scalar particles with no self–interaction. In order for axions to be an essential component of the dark matter content of the Universe, their mass should be $m \sim 10^{-5}$ eV. With this axion mass, the scalar field collapses forming compact objects with masses of order of $M_{\mathrm{crit}} \sim 0.6\, m_{\mathrm{Pl}}^2/m \sim 10^{-6}\,\mathrm{M}_\odot$ [44, 45], which corresponds to objects with the mass of a planet. Since the amount of dark matter in galaxies is ten times bigger than the luminous matter, we would need tenths of millions of such objects around the solar system, which is clearly not the case. Also, these candidates behave just like standard CDM, and then they cannot explain the observed scarcity of dwarf galaxies and the smoothness of the galactic-core matter densities. That is, they should behave as objects made of baryonic matter do, except that they do not emit light; in such case this type of stars should be distributed as luminous matter is. In one word, such scalar field stars have been proposed as dark matter simply because they could account for the total amount of matter in the whole universe, without taking care of the local effect like rotation curves.

Let us return to the SFDM hypothesis for a real scalar field Φ (for a complex counterpart picture, see [46]). If a galaxy is an oscillaton, i.e., an oscillating soliton object, it must correspond to coherent scalar oscillations around the minimum of the scalar potential (2). The scalar field Φ and the metric coefficients (considering the spherically symmetric case) would be time-dependent, though it has been shown that such a configuration can be stable, non-singular and asymptotically flat [44, 47, 48, 49, 50]. For the collapse of a real scalar field, the critical value for the mass of an oscillaton (the maximum mass for which a stable configuration exists) will depend on the mass of the boson. Roughly speaking, if we take $m_\Phi = 10^{-23}\,\mathrm{eV}$ (see (21)), and use the formula for the critical mass of the oscillaton corresponding to a scalar field with a Φ^2 potential (i.e. just a mass term), we expect the critical mass to be [44, 45, 50]

$$M_{\mathrm{crit}} \sim 0.6\,\frac{m_{\mathrm{Pl}}^2}{m_\Phi} \sim 10^{12}\,\mathrm{M}_\odot\,. \tag{23}$$

which means that the critical mass of the cosmological model depicted in Sect. 3 is of the order of magnitude of the dark matter content of a standard galactic halo.

The scenario of galactic formation we assume is the following. A sea of scalar field particles fills the Universe and forms localized primordial fluctuations that could collapse to form stable objects, which we will interpret as the dark matter halos of galaxies. The equations governing the evolution of such scalar galaxy halos correspond to the Einstein-Klein-Gordon (EKG) system, which we show below applied to the simplest case of spherical symmetry.

The spherically symmetric line element is written in the form

$$ds^2 = -\alpha^2(r,t)dt^2 + a^2(r,t)dr^2 + r^2 d\Omega^2\,, \tag{24}$$

with $\alpha(r,t)$ the lapse function and $a^2(r,t)$ the radial metric function, and where we have chosen the polar-areal slicing condition (i.e. we force the line element to have the above form at all times, so that the area of a sphere with $r = R$ is always equal to $4\pi R^2$). This choice of gauge will force the lapse function $\alpha(r,t)$ to satisfy an ordinary differential equation in r (see below). The energy momentum tensor of the scalar field is

$$T_{\mu\nu} = \Phi_{,\mu}\Phi_{,\nu} - \frac{1}{2}g_{\mu\nu}\left[\Phi^{,\sigma}\Phi_{,\sigma} + 2V(\Phi)\right]\,. \tag{25}$$

We now introduce the first order variables $\Psi = \Phi_{,r}$ and $\Pi = a\Phi_{,t}/\alpha$, with which the Hamiltonian constraint becomes

$$\frac{a_{,r}}{a} = \frac{1-a^2}{2r} + \frac{\kappa_0 r}{4}\left[\Psi^2 + \Pi^2 + 2a^2 V\right]\,, \tag{26}$$

and the polar-areal slicing condition takes the form:

$$\frac{\alpha_{,r}}{\alpha} = \frac{a_{,r}}{a} + \frac{a^2-1}{r} - \kappa_0 r a^2 V\,. \tag{27}$$

All other components of Einstein's equations either vanish, or are a consequence of the last two equations. The Klein-Gordon (KG) equation now reads

$$\Phi_{,t} = \frac{\alpha}{a}\,\Pi\,, \tag{28}$$

$$\Pi_{,t} = 3\frac{\partial}{\partial(r^3)}\left(\frac{r^2\alpha\Psi}{a}\right) - a\alpha\,\frac{\mathrm{d}V}{\mathrm{d}\Phi} \tag{29}$$

$$\Psi_{,t} = \left(\frac{\alpha\Pi}{a}\right)_{,r}\,. \tag{30}$$

Equations (26-30) form the complete set of differential equations to be solved numerically.

The study of the evolution of oscillatons is a very interesting field by itself and its description would deserve more space in this text [44, 47, 48, 49, 50]. However, we will focus our attention on the results related to the SFDM hypothesis and the non-linear collapse of density perturbations.

Fortunately, the collapse of scalar fluctuations under realistic conditions does not require the solution of the relativistic EKG system. We can make use of some approximations to show the promising features of the SFDM at galactic level.

4.1 The Flat Space-Time Approximation

In order to show some properties of scalar halos, we start by taking the simplest approximation, that is, the flat space-time approximation. A scalar field object (an oscillaton) in flat space-time contains a flat central density profile, as it seems to be the case in galaxies [47, 51]. In order to see this, we study a massive oscillaton with potential $V = \frac{1}{2}m_\Phi^2\Phi^2$ in the Minkowski background. Even though it is not a solution to the Einstein equations as we are neglecting the gravitational force provoked by the scalar field, the solution is analytic and helps us to understand some features that appear in the non-flat oscillatons.

Using spherical coordinates, the KG equation in the Minkowski spacetime reads

$$\Phi'' + \frac{2}{r}\Phi' - m_\Phi^2\Phi = \ddot{\Phi} \tag{31}$$

where over-dot denotes $\partial/\partial t$ and prime $\partial/\partial r$. The exact general solution for the scalar field Φ is

$$\Phi(t,r) = \frac{\mathrm{e}^{\pm \mathrm{i}kr}}{r}\mathrm{e}^{\pm \mathrm{i}\omega t} \tag{32}$$

from which we obtain the dispersion relation $k^2 = \omega^2 - m_\Phi^2$. For $\omega > m_\Phi$ the solution is non-singular and vanishes at infinity. We will restrict ourselves to this case. It is more convenient to use trigonometric functions and to write the particular solution in the form

$$\Phi(t,x) = \Phi_0 \frac{\sin(x)}{x} \cos(\omega t) \tag{33}$$

where $x = kr$. It oscillates in harmonic manner in time. The scalar field spreads over all space, i.e., it is not confined to a finite region, as we are neglecting the gravitational interactions.

The analytic expression for the scalar field energy density derived from (33) is

$$\varrho_\Phi = \frac{1}{2}{\Phi_0}^2 \left\{ \left[\left(\frac{x\,\cos(x) - \sin(x)}{x^2} \right)^2 - \frac{\sin^2(x)}{x^4} \right] k^4 \cos^2(\omega\, t) + \frac{\omega^2 k^2 \sin^2(x)}{x^2} \right\} \tag{34}$$

which oscillates with a frequency $2\omega t$. Observe that close to the central regions of the object, the density of the oscillaton behaves like

$$\varrho_\Phi \sim \frac{1}{2}{\Phi_0}^2 k^2 \left[\omega^2 - k^2 \cos^2(\omega\, t)\right] + O(x^2) \tag{35}$$

which implies that the density is almost constant in the central regions, i.e. when $x \to 0$ the central density oscillates around a fixed value.

On the other hand, the asymptotic behavior when $x \to \infty$, is such that $\varrho_\Phi \sim 1/x^2$, i.e., far away from the center, the flat oscillaton density profile behaves like that of an isothermal halo sphere (IHS): the mass function oscillates around $M \sim x$ at large distances from the center. Nevertheless, if the gravitational interaction is taken into account, the object must be confined[47] and the integrated mass of the scalar field gives a finite value. In Fig. 1 we show the comparison between the NFW, the IHS and a flat oscillaton for the same galaxy. Observe that the flat oscillaton and NFW profiles remain very

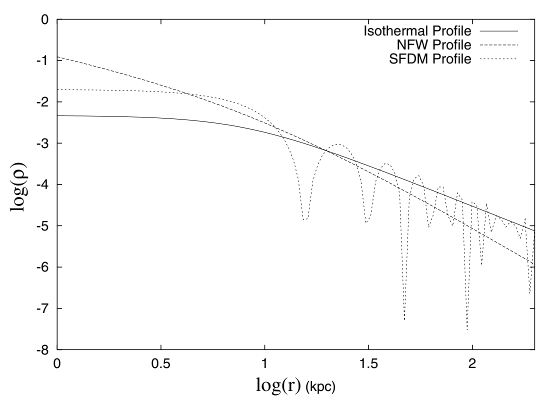

Fig. 1. Comparison between the energy density profile for the Scalar Field Dark Matter model with the NFW and the Isothermal models. The parameters for the isothermal model are $\rho_{\rm ISO} = 0.3/(r^2 + 8^2)$ and for the NFW profile are $\rho_{\rm NFW} = 10/(r(r+8)^2)$. The parameter used for the SFDM model are $k = 0.2$, $\sqrt{\kappa_0}\Phi_0 = 5 \times 10^{-2}$ in 33.

similar up to 100 kpc, then the flat oscillaton profile starts to follow the $1/r^2$ behavior, as the IHS one. The parameters used in the figures, correspond to a middle size galaxy.

As simple as the flat-spacetime approximation can be, it still shows that the density profile at the center of a scalar halo should be flat, as suggested by observations in galaxies. The self–gravity of the latter, if taken into account, will just change the profile at large distances from the center [47].

4.2 The Formation of Scalar Field Galaxy Halos

When the scalar field fluctuations reaches the non-linear regime, the scalar field collapses in a different way as the standard CDM. In a normal dust collapse, as for example in CDM, there is in principle nothing to avoid that the dust matter collapses all the time. There is only a radial gravitational force that provokes the collapse, and to stop it, one needs to invoke some virialization phenomenon.

In the scalar field paradigm the collapse is different. The radial and angular pressures are two natural components of the scalar field which prevent the collapse, avoiding the cusp density profiles in the centers of the collapsed objects (for details, see [50]). This is the main difference between the normal dust collapse and the SFDM one. The pressures play an important role in the SFDM equilibrium. In order to see this, as galaxies have an almost flat background, the Newtonian approximation of the EKG system (26-30) should be sufficient to understand them. This time, we will fully incorporate the influence of gravity in the process [52].

The weak field limit of the EKG equations arises when $\alpha^2 - 1, a^2 - 1, \sqrt{8\pi G}\,\Phi < 10^{-3}$ [45, 47]. We start by writing the scalar field and the metric coefficients in terms of the Newtonian fields ψ, U, U_2, A, A_2 as

$$\sqrt{8\pi G}\,\Phi = \mathrm{e}^{-\mathrm{i}\tau}\psi(\tau,x) + \mathrm{C.C.}\,, \tag{36}$$

$$\alpha^2 = 1 + 2U(\tau,x) + \mathrm{e}^{-2\mathrm{i}\tau}U_2(\tau,x) + \mathrm{C.C.}\,, \tag{37}$$

$$a^2 = 1 + 2A(\tau,x) + \mathrm{e}^{-2\mathrm{i}\tau}A_2(\tau,x) + \mathrm{C.C.}\,, \tag{38}$$

where we have also introduced the dimensionless quantities $\tau = mt,\ x = mr$. Notice that only U, A are real fields. Next, we assume that all the new fields are of order $\mathcal{O}(\varepsilon^2) \ll 1$, and that their derivatives obey the standard post-Newtonian rules $\partial_\tau \sim \varepsilon\partial_x \sim \mathcal{O}(\varepsilon^4)$. Therefore, considering the leading order terms only, the EKG equations now read

$$i\partial_\tau\psi = -\frac{1}{2x}\partial_x^2(x\psi) + U\psi\,, \tag{39}$$

$$\partial_x^2(xU) = x\psi\psi^*\,, \tag{40}$$

$$\partial_x U_2 = -x\psi^2\,. \tag{41}$$

In addition, $A(\tau,x) = x\partial_x U$ and $A_2 \sim \mathcal{O}(\varepsilon^4)$, that is, the metric coefficient g_{rr} can be taken plainly as time-independent.

It should be stressed here that the whole dynamics of the EKG system is contained in (39) and (40), which are the so-called Schrödinger–Newton (SN) equations[45, 46, 47, 53, 54, 55]; which also stand for the post-Newtonian expansion with complex scalar fields [45]. For example, under appropriate boundary conditions, stationary solutions of (39), (40) and (41) are in turn the so-called Newtonian oscillatons[47]. Indeed, (41) only arises for real scalar fields and represents the particular oscillatory behavior of the metric for oscillatons [44, 47, 49, 50].

For the initial data, we take the profile

$$\psi_i(0, x < x_0) = \psi_0 \frac{\sin(x/\sigma)}{(x/\sigma)}, \qquad (42)$$
$$\psi_i(0, x > x_0) = \psi_1 \frac{\exp\left[-\sqrt{2|U_0|\sigma^2 - 1}\,(x/\sigma)\right]}{x}.$$

where $(x_0/\sigma) \simeq (n+1)\pi < \sqrt{2|U_0|}x_0$, where $n = 0, 1, 2, ...$ labels the number of nodes of the initial profile, and $x_0 = mR_0$ with R_0 is the physical size of the initial matter fluctuation. ψ_1 is evaluated from the continuity condition of the radial function at $x = x_0$. This profile is the simplest we can imagine that depicts the expected characteristics of a realistic scalar fluctuation: a confined wave function with nodes. More details can be found in[52].

We mention here that SN system is invariant under the scaling transformation

$$\{\tau, x, U, U_2, \psi\} \to \left\{\beta^{-2}\hat{\tau}, \beta^{-1}\hat{x}, \beta^2\hat{U}, \beta^2\hat{U}_2, \beta^2\hat{\psi}\right\} \qquad (43)$$

where β is an arbitrary parameter. By means of (43) and an appropriate β, the collapse of our fluctuation can be reduced to the study of a conveniently sized configuration concerning *hat*-quantities only. Once the hat-configuration has been evolved, we apply the inverse transformation to recover the physical (no-hat) quantities.

We focus now on the numerical solution to the SN equations. Once the initial profile $\psi_i(0, x)$ is given, the Poisson equation (40) is integrated with a second order accurate upwind method inwards under the boundary condition $U(\tau, x_f) = GM(\tau, x_f)/x_f$ (being x_f the last point of our spherical grid), which is valid at each time slice according to the Newton theorems regarding spherical objects. The next scalar configuration is determined by solving the Schrödinger equation (39) using a second order finite differences fully implicit Cranck-Nicholson method [56]. The procedure is then repeated forward in time.

The accuracy depends on the time step $\Delta\tau$ and the grid resolution Δx, which should be chosen appropriately to assure that $|\Delta\psi|/|\psi| \ll 1$ in a time step. Thus, we should comply with both $\Delta\tau/(\Delta x)^2 \leq 1$ and $[\Delta\tau/(\Delta x)^2]|1 + U(\Delta x)^2| < 1$. The former is the condition applied to a free wave function, and the latter takes into account the presence of a potential in (39).

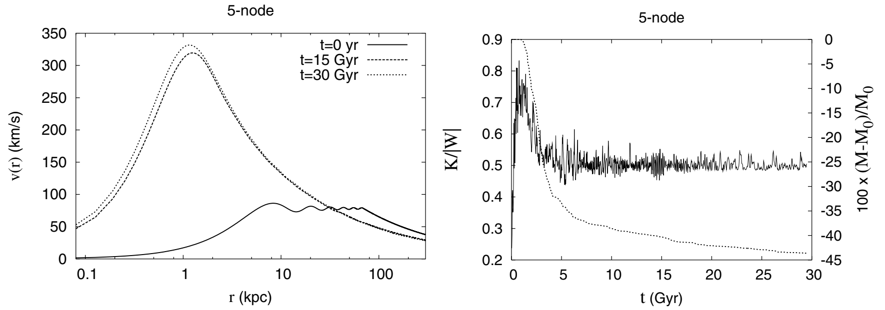

Fig. 2. Evolution of a 5-node initial scalar fluctuation of the form (42), see the text for details. Left: Profiles of the rotation curves $v(r) = \sqrt{GM(r)/r}$ at different times. Right: Evolution of the ratio Kinetic Energy/|Gravitational Potential Energy| (solid line), which shows the virialization of the two systems, and the total integrated mass M (dotted line). It is worth to notice the so called gravitational cooling after free fall of the system.

In Fig. 2 we show the run of an initial 5–node scalar fluctuation for a single scalar halo, whose initial physical parameters are $M_0 = 10^{11}\ M_\odot$ and $R_0 = 70$ kpc. The corresponding scale parameter is $\beta^2 = 6.38\times10^{-6}$, and then $\hat{\sigma} = 14.6$. The grid spacing is $\Delta\hat{x} = 0.25$ with the boundary at $\hat{x}_f = 1250$. The time step is $\Delta\hat{\tau} = 3\times10^{-2}$, and the run was followed up to a physical time of $T_0 = 30$ Gyr.

We see in Fig. 2 that the initial rotation curve profile is almost flat, but such flatness is lost at late times during the collapse. The scalar configuration rapidly virializes and forms a giant Newtonian oscillaton, almost as large as a realistic dwarf galaxy. The study of the SN system can be extended to the 3-dimensional case where the inclusion of a matter fluid is made through the r.h.s. of the Poisson equation (40). This issue will be reported elsewhere.

4.3 Supermassive Black Holes

It is worth to mention here that we can study the interaction between a scalar halo and a supermassive black hole at its center [57], as recent observations indicate is the case in real galaxies [42].

In this respect, for the SFDM hypothesis to survive, it should be shown that the central black hole does not represent a serious threat for the existence of a scalar halo. This is done, in first approximation, by solving the KG equation for a scalar field living in a fixed Schwarzschild background. This approximation is valid since the Schwarzschild radius of a typical supermassive black hole is smaller compared to the Compton length of a scalar particle of dark matter[7], $r_S \ll m_\Phi^{-1}$. The manifestation of the self-gravity of the scalar halo occurs at larger scales than m_Φ^{-1}.

[7] $r_S \simeq 10^{-13}\,(M_{bh}/M_\odot)$ pc.

From approximate analytical solutions of the KG equation, we can determine the fraction of incoming particles absorbed by the black hole (Γ), and the corresponding accretion rate of scalar matter. The results are, respectively,

$$\Gamma = 4\pi \left(m_\Phi r_\mathrm{S}\right)^3 \ , \tag{44}$$

$$\frac{\mathrm{d}M_\Phi}{\mathrm{d}t} = 4\pi \left(\Phi_0 m_\Phi r_\mathrm{S}\right)^2 \ , \tag{45}$$

where Φ_0 is the value of the scalar field (in units of $\kappa_0^{-1/2}$) near the horizon.

For typical values of the parameters involved, we get that $\Gamma \sim 10^{-20}$ and an accretion rate of around $10^{-14}\,M_\odot\,\mathrm{y}^{-1}$. This simple calculation shows that a scalar galaxy halo and a supermassive black hole can coexist.

5 Conclusions

In principle, it is possible to consider a braneworld model with an adequate Lagrangian in order to construct a consistent inflaton–dark matter scenario. The price we have to pay is that the inflaton remains after inflation and behaves as dark matter at the present epoch.

After inflation, the scalar dark matter we studied reproduces the success of the standard model of CDM, which seems to be correct at cosmological scales. We would like to stress that the SFDM gives the same results as the CDM model for both the homogeneous and the linearly perturbed cosmological evolutions.

On the non-linear realm of perturbations, we can track the evolution of scalar matter fluctuations through the use of numerical General Relativity. For the case of real scalar fields, scalar fluctuations collapse to form objects, called oscillatons, with a preferred mass of $\sim 10^{12}\,\mathrm{M}_\odot$. These objects are virialized and stable during periods of time longer than the actual age of the universe. Moreover, their density profiles are completely regular, i.e., without cusp centers, in a similar way as for real galaxies. This is encouraging enough [49, 58], to continue considering the scalar field as a good candidate to be the dark matter in the universe.

As a caution remark, we would like to mention that even if it is possible to identify the inflaton with the scalar field dark matter within braneworld models, this might not be necessarily the case. Despite the feasibility of the braneworld models, the results presented for epochs after inflation are still valid even if the dark matter scalar field were not fundamental. We should wait for more accurate observations to restrict the free parameters of the SFDM model and its relation to an inflationary epoch.

In conclusion, we have proposed a simple and unified model of inflationary dark matter, where the same scalar field provides the origin for the primordial spectrum of density perturbation (which are produced quantum–

mechanically) and later plays an important role evolving them to form the cosmological structures we observe today.

Acknowledgements

We would like to thank Aurelio Espíritu for technical suport. This work was partly supported by CONACyT México, under grants 32138-E and 34407-E and by a bilateral project DFG-CONACyT 444 MEX-13/17/0-1. The runs were made using the computer cluster in the Laboratorio de Supercómputo Astrofísico at Cinvestav-IPN, México.

References

1. N. A. Bahcall, J. P. Ostriker, S. Perlmutter and P. J. Steinhardt, Science **284**, 1481-1488. V. Sahni, A. Starobinsky, Int. J. Mod. Phys. D **9**, 373-444 (2000).
2. D. N. Spergel *et al*, `astro-ph/0302209`. J. L. Sievers *et al*, `astro-ph/0205387`.
3. A. R. Liddle and D. H. Lyth, *Cosmological inflation and large-scale structure* (Cambridge University Press, 2000). T. Padmanabhan, *Structure formation in the universe* (Cambridge University Press, 1993).
4. S. Perlmutter *et al. ApJ* **517** (1999)565. A. G. Riess *et al.*, *Astron.J.* **116** (1998)1009-1038.
5. J. Navarro, C. S. Frenk and S. S. M. White. ApJ **490**, 493 (1997).
6. W. J. G. de Blok, S. S. MacGaugh, A. Bosma and V. C. Rubin, ApJ **552**, L23 (2001). S. S. MacGaugh, V. C. Rubin and W. J. G. de Blok, ApJ **122**, 2381 (2201). W. J. G. de Blok, S. S. MacGaugh and V. C. Rubin, ApJ **122**, 2396 (2001).
7. J. J. Binney and N. W. Evans, *MNRAS* **327** L27 (2001). Blais-Ouellette, C. Carignan, and P. Amram, E-print astro-ph/0203146. C. M. Trott and R. L. Wesbster, E-print astro-ph/0203196. P. Salucci, F. Walter and A. Borriello, E-print astro-ph/0206304.
8. M. Kamionkowski and A. R. Liddle, Phys. Rev. Lett. **84**, 4525 (2000).
9. D. N. Spergel and P. J. Steinhardt, Phys. Rev. Lett. **84**, 3760 (2000); B. D. Wandelt, R. Dave, G. R. Farrar, P. C. McGuire, D. N. Spergel, and P. J. Steinhardt, astro-ph/0006344; C. Firmani, E. D'Onghia, V. Avila-Reese, G. Chincarini, and X. Hernández, MNRAS **315**, L29 (2000); C. Firmani, E. D'Onghia, G. Chincarini, X. Hernández, and V. Avila-Reese, MNRAS **321**, 713 (2001); M. Kaplinghat, L. Knox, and M. S. Turner, Phys. Rev. Lett. **85**, 3335 (2000).
10. N. Trentham, O. Moeller and E. Ramirez-Ruiz, MNRAS **322** 658 (2001).
11. F. S. Guzmán and T. Matos, Class. Quant. Grav. **17**, L9-L16 (2000). E-print gr-qc/9810028.
12. T. Matos and L. A. Ureña-López, Class. Quantum Grav. **17**, L75 (2000).
13. H. Dehnen and B. Rose, Astrophys. Sp Sci. **207** (1993) 133-144. H. Dehnen, B. Rose and K. Amer, Astrophys. Sp Sci. **234** (1995) 69-83.
14. P. J. E. Peebles, Astrophys. J. **534**, L127 (2000); J. Goodman, New Astron. **5**, 103 (2000). M. C. Bento, O. Bertolami, R. Rosenfeld, and L. Teodoro, Phys. Rev. D **62**, 041302 (2000); O. Bertolami, M. C. Bento, and R. Rosenfeld, astro-ph/0111415. A. Riotto and I. Tkachev, Phys. Lett. B **484**, 177 (2000).

15. C. Wetterich, Nucl. Phys. B **302**, 668 (1988); B. Ratra and P. J. E. Peebles, Phys. Rev. D **37**, 3406 (1988); E. J. Copeland, A. R. Liddle, and D. Wands, Phys. Rev. D **57**, 4686 (1998). R. R. Caldwell, R. Dave, and P. J. Steinhardt, Phys. Rev. Lett. **80**, 1582 (1998); L. Wang, R. R. Caldwell, J. P. Ostriker, and P. J. Steinhardt, Astrophys. J. **503**, 17 (2000).
16. L. A. Ureña-López and T. Matos, Phys. Rev. D **62**, 081302 (2000).
17. V. Sahni and L. Wang, Phys. Rev. D **62**, 103517 (2000).
18. P. G. Ferreira and M. Joyce, Phys. Rev. D **58**, 023503 (1998).
19. N. Arkani-Hamed, S. Dimopoulos and G. Dvali, *Phys. Lett.* **B 429**, 263 (1998); I. Antoniadis, N. Arkani-Hamed, S. Dimopoulos and G. Dvali, Phys. Lett. **B436**, 257 (1998).
20. L. Randall and R. Sundrum, *Phys. Rev. Lett* **83**, 3370 (1999); 4690 (1999).
21. G. Dvali, G. Gabadadze and M. Porrati, *Phys. Lett.* **B 484**, 112 (2000).
22. C. Deffayet, *Phys. Lett.* **B 502**, 199 (2001).
23. G. Dvali, G. Gabadadze, *Phys. Rev. D* **63**, 065007 (2001).
24. P. Binetruy, C. Defayyet, and D. Langlois *Nucl. Phys.* **B 565**, 269 (2000).
25. D. Ida, *JHEP* **0009**, 014 (2000).
26. N. Deruelle and T. Dolezel, *Phys. Rev. D* **62**, 103502 (2001).
27. P. Bowcock, C. Charmousis and R. Gregory, *Class. Quant. Grav.* **17**, 4745 (2000).
28. A. C. Davis, S. C. Davis, W. B. Perkins and I. R. Vernon, *Phys.Lett* **B 504**, 254 (2001).
29. E. J. Copeland, A. R. Liddle, and J. E. Lidsey, Phys. Rev. D **64**, 023509 (2001).
30. G. Huey and J. Lidsey, Phys. Lett. **B514**, 217 (2001).
31. V. Sahni, M. Sami, and T. Souradeep, Phys.Rev. D **65**, 023518 (2002).
32. J.E. Lidsey, T. Matos and L.A. Ureña-López, *Phys. Rev. D* **66** 023514 (2002).
33. H. García-Compeán, R. Cordero and T. Matos. To be published.
34. C. P. Burgess, A. de la Macorra, I. Maksymyk and F. Quevedo, *Phys. Lett.* **B 410** 181 (1997).
35. A. R. Frey and A. Mazumdar, *Phys. Rev. D* **67**, 046006 (2003). E-print hep-th/0210254.
36. R. Maartens, D. Wands, B. A. Basset, and I. P. C. Heard, Phys. Rev. D **62**, 041301 (2000).
37. L. H. Ford, Phys. Rev. D **35**, 2955 (1987); L. P. Grishchuk and Y. V. Sidorov, Phys. Rev. D **42**, 341 (1990); B. Spokoiny, Phys. Lett. B **315**, 40 (1993).
38. D. H. Lyth, and D. Wands, Phys. Lett. B**524**, 5 (2002). D. H. Lyth, C. Ungarelli, and D. Wands, E-print astro-ph/0208055. N. Bartolo and A. R. Liddle, Phys. Rev. D **65**, 121301(R) (2002). A. R. Liddle and L. A. Ureña-López, E-print astro-ph/0302054.
39. W. Hu, R. Barkana, and A. Gruzinov, Phys. Rev. Lett. **85**, 1158 (2000).
40. T. Matos and L. A. Ureña-López, Phys. Rev. D **63**, 063506 (2001).
41. T. Matos and L. A. Ureña-López, Phys. Lett. B **538**, 246 (2002).
42. L. Ferrarese, E-print astro-ph/0207050, astro-ph/0207050.
43. B. Moore, Nature **370**, 629 (1994). A. Burkert, ApJ **477**, L25 (1995). J. A. Tyson, G. P. Kochanski and I. P. Dell'Antonio, ApJ **498**, L107 (1998).
44. E. Seidel and W. Suen, Phys. Rev. Lett. **66**, 1659 (1991). E. Seidel and W. Suen, Phys. Rev. Lett. **72**, 2516 (1994).
45. E. Seidel and W-M. Suen, Phys. Rev. D **42**, 384 (1990); J. Balakrishna, E. Seidel, and W-M. Suen, Phys. Rev. D **58**, 104004 (1998).

46. A. Arbey, J. Lesgourgues, and P. Salati, Phys. Rev. D **64**, 123528 (2001); *ibid*, **65**, 083514 (2002); astro-ph/0301533.
47. L. A. Ureña-López, Class. Quantum Grav. **19**, 2617 (2002); L. A. Ureña-López, T. Matos, and R. Becerril, Class. Quantum Grav. **19**, 6259 (2002).
48. S. H. Hawley and M. W. Choptuik, Phys. Rev. **D 67**, 024010 (2003).
49. M. Alcubierre, F. S. Guzmán, T. Matos, D. Núñez, L. A. Ureña-López and P. Wiederhold. Class. Quantum Grav. **19**, 5017 (2002).
50. M. Alcubierre, R. Becerril, F. S. Guzmán, T. Matos, D. Núñez, and L. A. Ureña-López, E-print gr-qc/0301105.
51. T. Matos and D. Núñez, E-print astro-ph/0303455.
52. F. Siddhartha Guzmán and L.A. Ureña-López, Phys. Rev. D, in press. E-print astro-ph/0303440.
53. S. J. Sin, Phys. Rev. D **50**, 3650 (1994); S. U. Ji and S. J. Sin, Phys. Rev. D **50**, 3655 (1994).
54. J. W. Lee and I. G. Koh, Phys. Rev. D **53**, 2236 (1996).
55. R. Friedberg, T. D. Lee, and Y. Pang, Phys. Rev. D **35**, 3640 (1987). I. M. Moroz, R. Penrose, and P. Tod, Class. Quantum Grav. **15**, 2733 (1998); P. Tod and I. M. Moroz, Nonlinearity **12**, 201 (1999).
56. W. H. Press, S. A. Teukolsky, W. T. Watterling and B. P. Flannery, *Numerical Recipes in Fortran.* Cambridge University Press, 1992.
57. L. A. Ureña-López and A. R. Liddle, Phys. Rev. D **66**, 083005 (2002).
58. T. Matos and F. S. Guzmán, Class. Quantum Grav. **18**, 5055 (2001).